The structure and optical properties of Lithium Niobate grown on quartz for photonics application

Makram A. Fakhri[1*], *M.Halim* A. Wahid[2], *Suad* M. Kadhim[1], *Ban* A. Badr[3], *Evan* T. Salim[4], *Uda* Hashim[5] *and Zaid* T. Salim[5]

[1]Laser and Optoelectronic Department, University of Technology, 10001 Baghdad, Iraq
[2]Semiconductor Photonics & Integrated Lightwave Systems (SPILS), School of Microelectronic Engineering, University Malaysia Perlis, Pauh Putra Campus, Arau 02600 Malaysia
[3]Laser Science Branch, University of Technology, 10001 Baghdad, Iraq
[4]Institute of Nano Electronic Engineering, University Malaysia Perlis, 01000 Kangar, Perlis, Malaysia

Abstract. This paper focuses on the structure and optical properties of Lithium niobate (LN) deposited on quartz substrate by sol-gel method. The solution was prepared at different molarity concentration and annealed at 500 ºC. The LNs were analyzed by UV-visible, X-ray diffraction (XRD) and Scanning Electron Microscope (SEM). The results show that as the molar concentration increases, the films crystallization becomes more atomically distributed and the energy band gap approaches 4 eV. Transmission spectra were taken in the wavelength range of 400-1100 nm. Hexagonal structure was observed with good atoms distribution and homogeneous crystallization. There were two phases of LNs recorded in this work.

1 Introduction

Lithium Niobate (LiNbO3) has recently attracted photonics industries owing to its optical material properties such as electro optic and acoustic optic. These properties have been investigated and showed uniqueness thus became attractive candidate in the nanophotonics area [1, 2]. LiNbO3 single crystal is an excellent material for non-linear optics and electro-optics applications. It is one of the key materials for optical based technologies because of its large second-order nonlinearities [3]. Because of its remarkable linear and nonlinear optical properties, chemical and mechanical stability makes lithium niobate (LN) an attractive host material for application in photonic crystal devices [4]. Moreover LN has high electro-optical coefficient and low optical losses thus offers suitability in optical communication systems, which are widely used for applications in microwave telecommunications, memory units, electro optics, modulators, optical switches, waveguides, beam deflectors, second harmonic generation, surface acoustic waves (SAW) devices, parametric optical converters and data transmission [5-10].

LiNbO3 has hexagonal structure with lattice parameters a = 0.5147 nm and c = 1.3862 nm [11]. However, LiNbO3s have several potential advantages from technological or commercial view point of integrated optics [12]. Optical waveguides comprised of hetero-materials efficiently confine propagating light because of large difference in refractive indices between the film and the substrate [13]. Therefore, LiNbO3s have been grown by several techniques including liquid-phase epitaxy [14], Ion Beam Sputtering [15], RF magnetron sputtering [16], molecular beam epitaxy [17], metal–organic chemical vapor deposition [18], pulsed-laser deposition (PLD) [19], thermal plasma spray chemical vapor deposition [20], electron-cyclotron-resonance (ECR) plasma sputtering [21], electron beam irradiation [22] and pulsed laser ablation (PLA) [23].

In the present work, the effect of molarity concentration on the growth of LiNbO3 on quartz substrate was investigated. Generally the structure and optical behaviors was measured and analyzed in correspondent to variable molarity. Sol-gel method was utilized due to its simplicity, economic and adequately precise. Quartz was chosen as a substrate because of its compatibility with a wide variety of processing techniques and other optical properties like band gap, refractive index, extinction coefficient, dielectric constant and Urbach energy.

.

.

* Corresponding author: mokaram_76@yahoo.com

2 Methodology

The preparation procedure of $LiNbO_3$ was performed by mixing Nb_2O_5 (ultra-purity, 99.99%) and citric acid (CA) without further purification. The solution was added into Li_2CO_3 and Ethylene Glycol. The molar ratio between Li_2CO_3 and Nb_2O_5 was the same as to maximize the formation of $LiNbO_3$ stoichiometry phase. Firstly, the $LiCO_3$, Nb_2O_5, and citric acid was dissolved in Ethylene Glycol with heating and stirring at 90 ºC for 48 hr. The obtained solution was directly deposited on quartz substrate of 1×1 cm^2 at 3000 rpm for 30 sec. After each coating, the film was dried in air at 120 °C for 10 min and was calcined at 250 °C for 1 h to remove the organics. The process was performed several times until the desired film thickness was achieved. Finally, the films were annealed at 500 °C for 2 hr. The prepared film was clear, transparent, white to brown color and has a good adhesive properties and smooth surface. After that it was calcined at 500 ºC for 2 hr in static air and oxygen atmosphere to remove the organics. The optical properties were measured via transmittance (T) spectrum in the range of 300-1100 nm double-beam Ultr-Violet (UV-vis) spectrophotometer (Shimadzu UV-Vis 1800, Japan). The incident photon energy was calculated as a function of wavelength (λ) by using [24]

$$E_g(eV)=1240/\lambda(nm) \quad (1)$$

where λ is wavelength. The energy dependence of absorption coefficient (α) near the band edge for band to band and excition transition could be described by Tauc formulas [25]

$$(\alpha hv)=B(hv-E_g)r \quad (2)$$

where B is a constant inversely proportional to amorphous, r is constant equals 2, 3, 1/2, 3/2 depending on the material and the type of the optical transition αhv. If the straight portion of the plot of $(\alpha hv)^{1/r}$ against (hv) is extrapolated to $(\alpha hv)^{1/r}=0$, the intercept gives the energy gap value. The absorption coefficient (α) for each wavelength was calculated by [26]

$$\alpha=2.303(A/t) \quad (3)$$

where A is absorbance and t is transmittance.

The structural evolution of the as-prepared nanostructures was examined using high-resolution X-ray diffraction (HR-XRD), equipped with Cu-Kα-radiation of wavelength λ = 0.15418 nm at 40 kV and 30 mA. The thickness of the annealed samples was studied using scanning optical reflectometer while the surface structure was monitored by the scanning electron microscopy (SEM).

3 Results and discussion

3.1 Optical properties

The transmission spectra of $LiNbO_3$ nanophotonics films at different molarities concentrations are shown in Fig. 1. It was found that the transmission decreased as molarities concentration increased due to increment in deposition rate and structural thickness. The values of transmission were ranged between 48-96% with molarities concentration of 1.00 to 0.1 mol/L, similar results were found in other work [27]. The lower value of transmittance is attributed to excessive $LiNbO_3$ ions existing at interstitial sites that probably absorb the light. The moderately high transmittance throughout UV-Vis regions makes a good material for optoelectronics application.

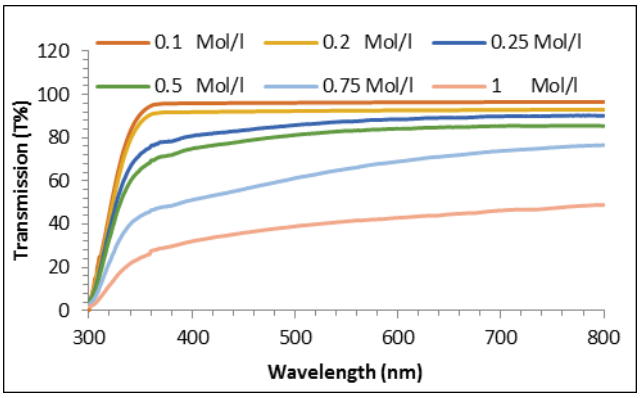

Fig. 1. Transmission spectra of $LiNbO_3$ nanostructures prepared at different molarities concentration

The optical reflectance (R %) of $LiNbO_3$ nanophotonics was measured using double-beam UV-vis instrument. Fig. 2 shows the reflectance of $LiNbO_3$ nanophotonics films within the wavelength range of 300-700 nm at room temperature. It's clearly observed that optical reflection increased with molar concentration. This is due to the fact that when a beam of light illuminates on a dielectric thin film the light ray is partially reflected and transmitted, depending on energy of incident photon and film thickness since the prepared material consists of charged particles, bound and loose electrons, ionic elements, etc.

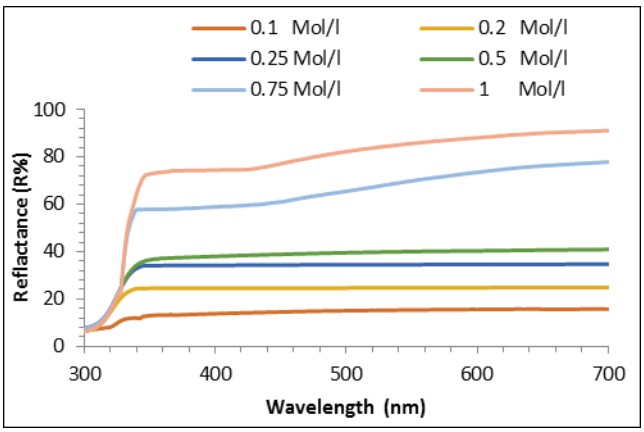

Fig. 2. Reflection spectra of $LiNbO_3$nanostructures prepared at different molarities concentration

At infrared and visible light frequencies, the contribution comes only from the displacement of the electron. In dielectric solids, there is a specific energy separating the valence band and the conduction band, known as the energy band-gap. It values were estimated and found by a plot as shown in Fig. 3. It could be shown that the band gap increases with the molarities concentration due to decreases in material grain size. In dielectrics materials the main absorption process resulting from the interaction of optical radiation and the electrons. If the energy of the incident light beam equals to the energy required in exciting an electron to the higher energy level, the photon may be absorbed taking into account that the electron may be free electron or core electron in the materials. In case of $LiNbO_3$, in the visible region no excitation can accrue, since the electrons are tightly restricted that the energy in the ultraviolet region is required. The obtained results are synchronized with experimental value in other work [24].

In the field of optical thin films deposition, the light wavelength is mostly larger than inter atomic distance. Therefore the light wave interaction with the materials are middling over a lot of unit cells. As a result, the optical properties within thin films could be depicted by using optical parameters or optical constants.

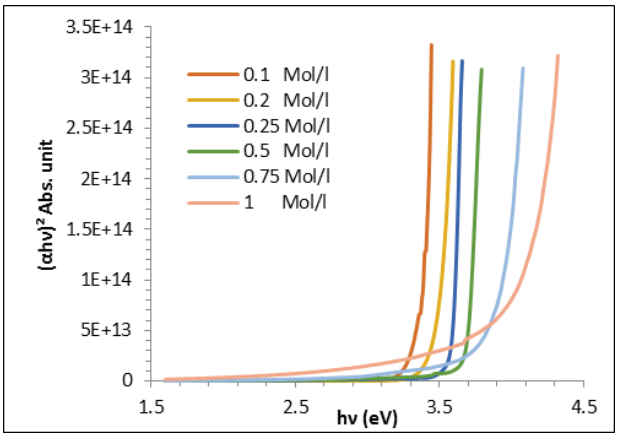

Fig. 3. Energy band gap of $LiNbO_3$ in different molar concentrations

3.2 Structural properties

The XRD result of $LiNbO_3$ nanostructures deposited on quartz substrates grown by sol–gel method is shown in Fig. 4. The XRD pattern was obtained from $LiNbO_3$ thin films deposited on quartz substrates at optimum condition (1Ml/L).The crystal structure of $LiNbO_3$ nanostructures is found to have hexagonal structure. It is observed that the peaks at 2θ = 23.634, 32.637, 34.674, 48.355, 53.106, and 55.879 correspond to (012), (104), (110), (024), (116) and (122) planes. Hence, the crystal structure will be more crystallized with higher molarity concentration. All the reflection peaks could be indexed to the hexagonal structure with lattice parameters a = 5.145, c= 13.858, which were very close to the reported data in the A.Z. Simoes et al [28]. The thin film remained polycrystalline structure after annealing at 500 ^{0}C for 2 h in static air. Two phases of Lithium niobate could be recognized which is Δ and δ phases. It is noted that a preferred Δ phase exists in the film and performed orientation of (012). The XRD clearly indicates the presence of a small amount of secondary Li deficient phase ($LiNb_3O_8$) at all molar concentrations. This phase is originated from an interface reaction between the Oxygen and $LiNbO_3$. The phase could be detected by XRD owing to its high crystallization temperature and observed at peaks 2θ = 24.407, 30.262 and 35.981 correspond to (400), (410) and (212) planes. This is attributed to annealing effect in static air and oxygen atmosphere. There was an impurity site of Nb_2O_5 at peaks 2θ = 24.433 and 31.623 which correspond to (-105) and (014) planes. The planes of Nb_2O_5 were not considered as a major plane that may change our observation significantly.

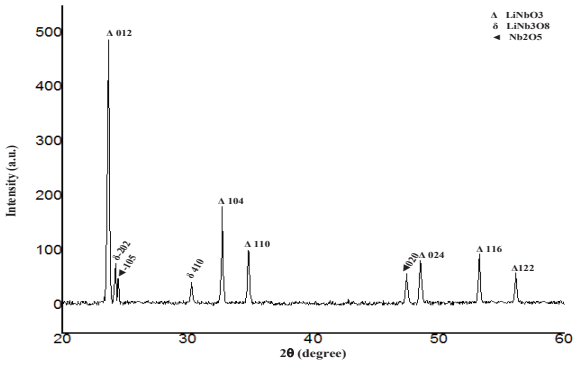

Fig. 4. XRD spectra of $LiNbO_3$ in optimum condition of higher molarity concentration (1 Mol/L)

3.3 Morphological studies

It is an interesting parameter for integrated-optic and optoelectronic applications. Figure 5 shows SEM images (5x5 μm) of $LiNbO_3$ nanostructures deposited on quartz substrates at different molarity concentrations. The density of nucleation for the $LiNbO_3$ thin films was not uniform on the flat substrate. Higher molarity concentration (optimum condition) depicts more homogenousity and leads to a better distribution than the lower molar concentration level. As discussed earlier, this suggests that higher molarity concentration directs the $LiNbO_3$ nanostructures toward regular spread.

An overview image at low magnification illustrates that the obtained samples are quite uniform in shape. A closer examination of these samples indicates that our synthesized film like ice layers shape of morphology.

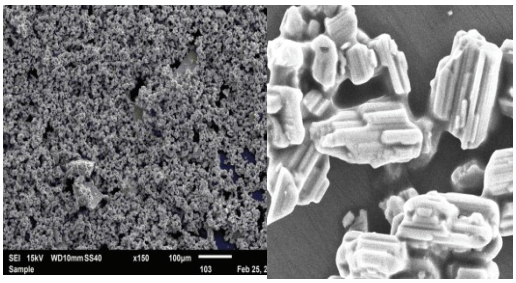

(a) (b)

Fig. 5. Surface morphology of $LiNbO_3$ nanostructures at optimum condition of molarity concentration (a) 1 Mol/L at high magnification, (b) 1 Mol/L at low magnification

4 Conclusion

The $LiNbO_3$ nanostructures have been chemically prepared by spin-coating technique. SEM images elucidate that the nanostructures will be more homogenous as the molarity concentration increases. Based on XRD results, the $LiNbO_3$ nanostructures have polycrystalline in nature. The highest intensity is shown at orientation (012) at $2\theta = 23.634$, a significant increment at the spin coating speed of 3000 rpm. As expected, the structure is more crystalline with higher molar concentration. Optical properties analysis provides energy band gap values between 2.88 to 3.975 eV for different molarity concentrations.

References

1. D. Janner, D. Tulli, M. Jofre, D. Yudistira, S. Balsamo, M. Belmonte, and V. Pruneri, IEEE Journal of Selected Topics in Quantum Electronics,**19**, 34006-34016, (2013).
2. Makram A Fakhri, Y Al-Douri, U Hashim, Evan T Salim, Solar Energy, **120**: 381-388, (2015).
3. P. Kumar, S.M. Baru, S Perero, R.M.L.Sai, I Bhamik, S. Ganesamoorthy, A.K. Karnal, J. Phys. **75**, 1035-1040, (2010).
4. M.R.R. Gesualdi, C. Jacinto, T. Catunda, M. Muramatsu, V. Pilla, Appl. Phys. B, **93** , 879–883 (2008).
5. Marwa Abdul Muhsien,Evan T. Salem, Ibrahim R. Agool, Haidar Hamed Hamdan, Applied Nanoscience **4**: 719–732 (2014).
6. M.-P. Bernal, N. Courjal, J. Amet, M. Roussey, C.H. Hou, Optics Communications **265**, 180–186 (2006).
7. V. Ievlev, M. Sumets, A. Kostyuchenko, N. Bezryadin, J Mater Sci: Mater Electron **24** , 1651–1657 (2013).
8. H-S. Jung, Journal of the Optical Society of Korea **16**, 47-52 (2012).
9. Makram A. Fakhri, Y. Al-Douri, U. Hashim, E.T. Salim, D. Prakash, K. D. Verma, Applied Physics B **121**: 107–116 (2015).
10. D. Janner1, D.Tulli , M. Garc´ıa-Granda, M. Belmonte, and V.Pruneri, Laser & Photon. Rev **3**, 301–313 (2009).
11. V. Ievlev , V. Shur , M. Sumets and A. Kostyuchenko, Acta Metallurgica Sinica (English Letters) **26**, 630-634, (2013).
12. N. E. Stankovaa, S. H. Tonchevb, E. Gyorgyc, G. Socolc, I. Mihailescuc, Journal of Optoelectronics and Advanced Materials **6**, 1345 – 1348, (2004).
13. Ch. Wang,M. J. Burek, Z. Lin, H. A. Atikian, V. Venkataraman, I. Huang, P. Stark and M. Lončar, OPTICS EXPRESS **22**, 30924-30933, (2014).
14. C. Dubs , J-P. Ruske , J. Krulich , A. Tünnermann, Optical Materials **31**, 1650–1657, (2009).
15. Makram. A. Fakhri, Y. Al-Douri, Uda. Hashim, Evan. T. Salim, Australian Journal of Basic and Applied Sciences **9,** 128-133, (2015).
16. V. Ievlev, M. Sumets, A. Kostyuchenko, N. Bezryadin, Journal of Materials Science: Materials in Electronics **24**, 1651-1657, (2013).
17. Abdulhadi Kadhim, Evan T. Salim, Saeed M. Fayadh, Ahmed A. Al-Amiery,Abdul Amir H. Kadhum, and Abu Bakar Mohamad, *The Scientific World Journal*, Article ID 490951, 6 paes, (2014).
18. Y. Akiyama, K. Shitanaka, H. Murakami, Y-S. Shin, M, Yoshida, N.Imaishi, Thin Solid Films **515**, 4975–4979, (2007).
19. Ji-Won Son, Sergei S. Orlov, Bill Phillips, Lambertus Hesselink, Journal of Electroceramics **17**, 591-595, (2006).
20. Makram A. Fakhri, U. Hashim, Evan T. Salim, Zaid T. Salim, J Mater Sci: Mater Electron **27**, 13105–13112, (2016).
21. H. Akazawa, M. Shimada, Vacuum **80**, 704–707, (2006).
22. M.R. Beghoul , A. Boudrioua , R. Kremer , M.D. Fontana , B. Fougere , C. Darraud , J.C. Vareille , P. Moretti, Optical Materials **31**, 136–142, (2008).
23. F. Meriche, A. Boudrioua, R. Kremer, E. Dogheche, E. Neiss-Clauss, R. Mouras, A. Fischer M-R. Beghoul, E. Fogarassy, N. Boutaoui, Optical Materials **32**,1427–1434, (2010).
24. Evan T. Salem, Ibrahim R. Agool, Marwa Abdul Muhsien, International Journal of Modern Physics B **25**, 3863-3869, (2011).
25. N. Ghobadi, Ghobadi International Nano Letters **3**, 2-4, (2013).
26. M. Caglar , Y. Caglar, S. Ilican, Journal of optoelectronics and advanced materials **8**, 1410 – 1413, (2006).
27. S. Ilican , Y. Caglar , M. Caglar , F. Yakuphanoglu, Applied Surface Science **255**, 2353–2359, (2008).
28. A.Z. Simoes, M.A. Zaghetea, B.D. Stojanovica, C.S. Riccardi, A. Ries, A.H. Gonzaleza, J.A. Varelaa, Materials Letters **57** , 2333 – 2339, (2003).